

Inter and intramolecular interactions and rotational tunneling of methyl groups in tetramethyltin

Da Zhang, Michael Prager, and Alarich Weiss

Citation: *The Journal of Chemical Physics* **94**, 1765 (1991); doi: 10.1063/1.459950

View online: <http://dx.doi.org/10.1063/1.459950>

View Table of Contents: <http://scitation.aip.org/content/aip/journal/jcp/94/3?ver=pdfcov>

Published by the [AIP Publishing](#)

Articles you may be interested in

[The physics of rotational tunneling: hole-burning spectroscopy of methyl groups](#)

Low Temp. Phys. **32**, 1020 (2006); 10.1063/1.2389008

[A combined nuclear dynamics and electronic study of the coupling between the internal rotation of the methyl group and the intramolecular proton transfer in 5-methyltropone](#)

J. Chem. Phys. **117**, 7525 (2002); 10.1063/1.1503317

[Methyl group rotational tunneling splittings and spin conversion dynamics: p-chlorotoluene in cyclohexane](#)

J. Chem. Phys. **117**, 4639 (2002); 10.1063/1.1504432

[Calculation of rotational tunneling states of the methyl group in the higher order of potential](#)

AIP Conf. Proc. **256**, 511 (1992); 10.1063/1.42424

[Hindered Rotation of the Methyl Groups in Ethane](#)

J. Chem. Phys. **4**, 749 (1936); 10.1063/1.1749784



Inter- and intramolecular interactions and rotational tunneling of methyl groups in tetramethyltin

Da Zhang^{a)}

Institut für Physikalische Chemie, Physikalische Chemie III, Technische Hochschule Darmstadt, Petersenstrasse 20, Darmstadt D-6100, Germany

Michael Prager

Institut für Festkörperforschung, Forschungszentrum Jülich Postfach 1913, Jülich D-5170, Germany

Alarich Weiss

Institut für Physikalische Chemie, Physikalische Chemie III, Technische Hochschule Darmstadt, Petersenstrasse 20, Darmstadt D-6100, Germany

(Received 2 July 1990; accepted 10 October 1990)

Rotational tunneling of methyl groups in partially deuterated tetramethyltin compounds, $(\text{CH}_3)_x\text{Sn}(\text{CD}_3)_{4-x}$ with $x = 1$ and 3 , and in various isotopic mixtures, $[(\text{CH}_3)_4\text{Sn}]_x[\text{Sn}(\text{CD}_3)_4]_{1-x}$, $x = 0.027, 0.20$, and 0.50 , and $[\text{CH}_3\text{Sn}(\text{CD}_3)_3]_x[\text{Sn}(\text{CD}_3)_4]_{1-x}$, $x = 0.10$, respectively, has been studied using the inelastic neutron-scattering (INS) technique. Compared with the INS spectrum of fully protonated tetramethyltin, $(\text{CH}_3)_4\text{Sn}$, the spectra obtained in the present study show remarkable shifts and broadenings or splittings of tunnel lines. The interpretation of the INS results is based on the assumption that all partially deuterated compounds and isotopically mixed systems have the same crystal structure as pure $(\text{CH}_3)_4\text{Sn}$. Combining the INS results with a detailed discussion of the crystal structure, all features can be explained in terms of both the intra- and intermolecular interactions of methyl groups. The overall decrease of tunnel splittings with deuteration is explained by the reduction of the lattice parameter and the increased octopole moment of the CD_3 groups. The interaction between different molecules is mediated by a subset of methyl group pairs only.

I. INTRODUCTION

The dynamics of molecular systems has been the subject of increasing interest over the past years and numerous studies have been reported. In particular, the rotational motions of simple, highly symmetric molecules and ions such as the ammonium ion, NH_4^+ , and the methane molecule, CH_4 , was and is intensively studied.¹⁻⁴ On the other hand, the methyl group attached to an organic or metal organic radical has attracted increasing interest because of the simple one-dimensional character of its rotation and because of the large variety and chemical variability of compounds containing methyl groups. The quantum character of this dynamics at low temperature was the most fascinating aspect of these studies.

The rotational dynamics is fully determined by the rotational potential of the molecule. The rotational potential a methyl group experiences in the solid state results from both intra- and intermolecular interactions. In some cases, the potential barriers may be rather low. A characteristic energy for rotational potentials is the tunnel splitting of the methyl groups, which is very sensitive to the potential strength and thus to changes of the intra- and intermolecular interactions. The inelastic neutron-scattering technique (INS) allows the direct observation of rotational tunneling transition of a methyl group at low temperature.^{5,6} Other experimental techniques were also applied intensively to study methyl group rotation, e.g., infrared spectroscopy, FIR,⁷ $^1\text{H-NMR}$

line-shape investigations [second moment $M_2(^1\text{H})$],^{8,9} and measurements of the spin-lattice relaxation of $^1\text{H-NMR}$ [$T_1(^1\text{H})$].¹⁰⁻¹² Because of their "spherical" shape, resulting from the high molecular symmetry, and the systematic increase of the intramolecular distances with exchange of the central atom M , the tetramethyl compounds of the group-IVa, $(\text{CH}_3)_4M$, $M = \text{C, Si, Ge, Sn, and Pb}$, have been a favored subject for the study of the rotational dynamics of the CH_3 groups and for the overall rotation of the molecule.^{7,11,13} Müller-Warmuth and coworkers^{11,14,15} studied the tunnel splittings of methyl groups in $(\text{CH}_3)_4M$, $M = \text{Si, Ge, Sn, and Pb}$ by INS and $T_1(^1\text{H})$ at low temperatures.

In the case of $(\text{CH}_3)_4\text{Sn}$, the INS spectrum shows two tunnel peaks with an intensity ratio of 1:3. It is known from the crystal structure^{14,16} that the tetramethyltin molecule in the solid state is distorted from its gas phase symmetry $\bar{4}3m$. The site symmetry of the molecule in the lattice is a threefold axis. Thus the tunneling transitions can be assigned to crystallographically inequivalent methyl groups within one molecule. A finite width of the strong tunneling transitions was tentatively attributed to coupling effects.

Analogously to $(\text{CH}_3)_4\text{Sn}$ the tunnel spectrum of $(\text{CH}_3)_4\text{Pb}$ shows two splittings, too, with the same intensity ratio. It was interpreted with the same model used for $(\text{CH}_3)_4\text{Sn}$, despite the lack of knowledge of the crystal structure of tetramethyl lead.¹⁵ However, the assumption of isomorphism for $(\text{CH}_3)_4M$, $M = \text{Sn, Pb}$, is a rather safe one and it is implicitly proved by the general shape of the tunneling spectrum.

Up to now, the studies^{7,11,13} of rotational potentials of

^{a)} Part of Dr.-Ing. Dissertation of Da Zhang, D17, Technische Hochschule Darmstadt, Germany.

methyl groups in $(\text{CH}_3)_4M$ compounds have focused mainly on systematic changes of their properties, such as packing or intramolecular contributions to the potential strength with the change of the center atom M . Especially the torsional frequencies of the methyl group and the energy barrier to methyl group reorientation were related with change of the molecular diameter and the bond length $d(M-C)$. For a long time it was assumed that the intermolecular van der Waals interactions $\text{CH}_3 \leftrightarrow \text{CH}_3$ are almost negligible. The intramolecular methyl-methyl interaction was taken as the very dominant part of the rotational potential of the methyl group.¹¹

In this context an interesting experiment was reported by Prager and Langel.¹⁷ The authors embedded molecules $(\text{CH}_3)_4\text{Sn}$ in a matrix of rare gases, Ar and Kr, respectively. The tremendous effect of such an isolation experiment is obvious from the INS spectrum: (1) the four methyl groups within one molecule now become equivalent—only one tunnel peak appears; and (2) the rotational potential is drastically reduced—the tunnel splitting is now at $h\nu_t = 72.0 \mu\text{eV}$, which has to be compared with pure $(\text{CH}_3)_4\text{Sn}$, $h\nu_t = 1.72 \mu\text{eV}$ and $13.3 \mu\text{eV}$. Thus, clearly, the intermolecular interactions contribute to the rotational potential comparably to the intramolecular ones.

The experimental evidence on tunneling motions in compounds $(\text{CH}_3)_4M$, $M = \text{Si}, \text{Ge}, \text{Sn}$, and Pb available up to now suggested the “pseudo” matrix experiments we report here: INS on partially deuterated tetramethyltin, that is, on $(\text{CH}_3)_n\text{Sn}(\text{CD}_3)_{4-n}$, $n = 1, 3$, and on mixtures $[(\text{CH}_3)_4\text{Sn}]_x[\text{Sn}(\text{CD}_3)_4]_{1-x}$, $x = 0.027, 0.20, 0.50$, and $[(\text{CH}_3\text{Sn}(\text{CD}_3)_3)_x[\text{Sn}(\text{CD}_3)_4]_{1-x}]$, $x = 0.10$, respectively. Depending on the deuteration—partial deuteration or solution—the intra- and intermolecular contributions to the rotational potential are modified differently. Thus an analysis of the response of the system on deuteration can yield a detailed insight into the interaction in tetramethyl metal compounds. Tetramethyltin is particularly suitable for such experiments since:

(a) All tunnel splittings of methyl groups are in the range of the high-resolution backscattering spectrometer ($\delta E = 0.4 \mu\text{eV}$).

(b) The crystal structure of $(\text{CH}_3)_4\text{Sn}$ is roughly known, which is necessary for a more thorough interpretation of the INS spectrum. This is especially valid if there are crystallographically different methyl groups present.^{14,18-21} It can be assumed safely, that the systems $(\text{CH}_3)_n\text{Sn}(\text{CD}_3)_{4-n}$ and $[(\text{CH}_3)_4\text{Sn}]_x[\text{Sn}(\text{CH}_3)_4]_{1-x}$ crystallize within the $(\text{CH}_3)_4\text{Sn}$ structure.

(c) The reduced molecular symmetry of $(\text{CH}_3)_4\text{Sn}$ in the solid state, $3m$, in contrast to the $\bar{4}3m$ symmetry of the isolated molecule, yields an especially rich tunnel spectrum that contains sensitive information on intra- and intermolecular contributions to the rotational potential.

(d) Because of the different incoherent neutron-scattering cross sections of hydrogen and deuterium the CD_3 groups will not mask the INS of the CH_3 groups. CD_3 groups act as dilution.

(e) Besides the diluting effects, CD_3 groups modify the rotational potential of neighboring CH_3 groups due to their

strong octopole moment and smaller diameter.²²⁻²⁵ The changes are rather tiny and all features of the tunneling spectra will be kept in the energy range accessible to the spectrometer used.

II. EXPERIMENTAL

A. Sample preparation

The partially and fully deuterated tetramethyltin compounds, $(\text{CH}_3)_n\text{Sn}(\text{CD}_3)_{4-n}$, $n = 0, 1$, and 3 , were synthesized by Grignard reactions using methyl iodide- d_3 (Aldrich) and tin (IV) tetrachloride, methyltin tribromide, and trimethyltin bromide, respectively. The technique described in the literature²⁶ was applied with some small modifications.²⁷

All obtained partially and fully deuterated tetramethyltin compounds were purified by repeated distillations using a Micro spinning band column. The purity of the compounds was monitored by measuring the mass densities before and after distillation. The distillation was repeated until the mass densities remained constant.

Because there exist different values of the mass density of $(\text{CH}_3)_3\text{Sn}$ in the literature, the mass densities of $(\text{CH}_3)_4\text{Sn}$, $(\text{CH}_3)_3\text{SnCD}_3$, and $\text{CH}_3\text{Sn}(\text{CD}_3)_3$ were measured in the temperature range $15 < T < 60$,²⁷ respectively; the results are shown in Fig. 1. The mass densities ρ (g cm^{-3}) for these three compounds can be described as a function of temperature by

$$\rho = A - BT/^\circ\text{C}. \quad (1)$$

For $(\text{CH}_3)_4\text{Sn}$: $A/\text{g cm}^{-3} = 1.33730$; $B/\text{g cm}^{-3} \text{ } ^\circ\text{C}^{-1} = 1.814 \times 10^{-3}$. For $(\text{CH}_3)_3\text{SnCD}_3$: $A/\text{g cm}^{-3}$

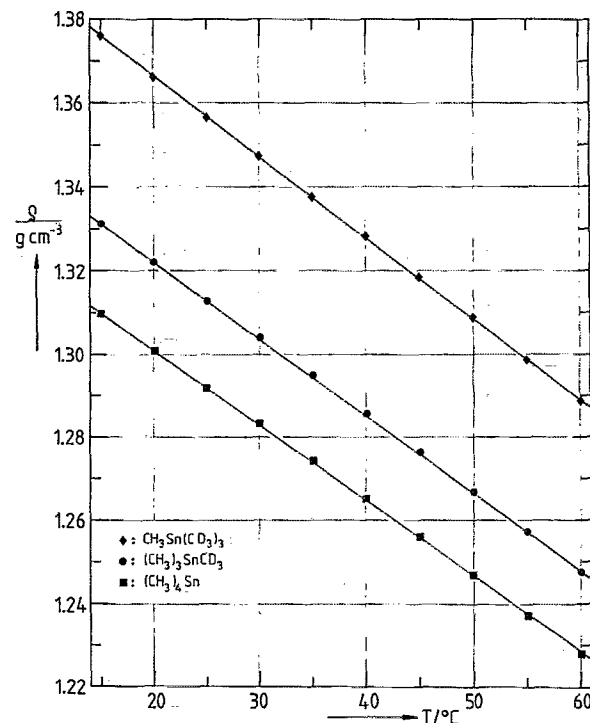


FIG. 1. Mass densities of $(\text{CH}_3)_4\text{Sn}$, $(\text{CH}_3)_3\text{SnCD}_3$, and $\text{CH}_3\text{Sn}(\text{CD}_3)_3$ measured by precision mass density instrument (Heraeus Paar DMA 02C) in the temperature range $15 < T/^\circ\text{C} < 60$.²⁷

$= 1.359\ 34$; $B/\text{g cm}^{-3}\text{ }^\circ\text{C}^{-1} = 1.853 \times 10^{-3}$. For $\text{CH}_3\text{Sn}(\text{CD}_3)_3$: $A/\text{g cm}^{-3} = 1.405\ 40$; $B/\text{g cm}^{-3}\text{ }^\circ\text{C}^{-1} = 1.935 \times 10^{-3}$. At $T = 25\text{ }^\circ\text{C}$ ρ_{exp} are given explicitly as $\rho[(\text{CH}_3)_4\text{Sn}] = 1.291\ 74\ \text{g cm}^{-3}$, $\rho[(\text{CH}_3)_3\text{SnCD}_3] = 1.312\ 81\ \text{g cm}^{-3}$, and $\rho[\text{CH}_3\text{Sn}(\text{CD}_3)_3] = 1.356\ 74\ \text{g cm}^{-3}$. The preparation of trimethyltin bromide, $(\text{CH}_3)_3\text{SnBr}$ is described elsewhere.¹⁸ The preparation of methyltin tribromide was carried out as follows:²⁸ KOH was dissolved in a 100-ml EtOH/H₂O mixture. $\text{SnCl}_2 \cdot 2\text{H}_2\text{O}$ was given to the alkaline solution under stirring. After cooling the solution was filtered. CH_3I was added to the filtrate and a stream of CO_2 was conducted through the solution over night. Methyl stannic acid, CH_3SnOOH , precipitated as a white powder and was separated from the solvent. The crude solid was mixed without further purification with HBr. After extraction with chloroform, the product, CH_3SnBr_3 , was recrystallized from CHCl_3 , mp: $53\text{ }^\circ\text{C}$ (Ref. 28: $53\text{ }^\circ\text{C}$).

B. Inelastic neutron-scattering experiment

The high-resolution INS spectra have been measured at the backscattering spectrometer IN10 of the Institute Laue-Langevin (ILL), Grenoble. An energy range $|E| < 14.6\ \mu\text{eV}$ was covered with a resolution $\delta E = 0.4\ \mu\text{eV}$ full width at half maximum. All INS measurements were carried out at $T = 4\ \text{K}$.

The following samples were studied: I. tetramethyltin- d_3 , $(\text{CH}_3)_3\text{SnCD}_3$; II. tetramethyltin- d_9 , $\text{CH}_3\text{Sn}(\text{CD}_3)_3$; III. mixture $[\text{CH}_3\text{Sn}(\text{CD}_3)_3]_{0.10}[\text{Sn}(\text{CD}_3)_4]_{0.90}$; IV. mixture $[(\text{CH}_3)_4\text{Sn}]_{0.027}[\text{Sn}(\text{CD}_3)_4]_{0.973}$; V. mixture $[(\text{CH}_3)_4\text{Sn}]_{0.20}[\text{Sn}(\text{CD}_3)_4]_{0.80}$; VI. mixture $[(\text{CH}_3)_4\text{Sn}]_{0.50}[\text{Sn}(\text{CD}_3)_4]_{0.50}$; VII. $(\text{CH}_3)_4\text{Sn}$, given for comparison.

III. RESULTS

The high-resolution INS spectra of the six sample (I–VI) studied in this paper are shown in Figs. 2–7, where the scattering function is $S(Q, \omega)$, Q is the momentum transfer

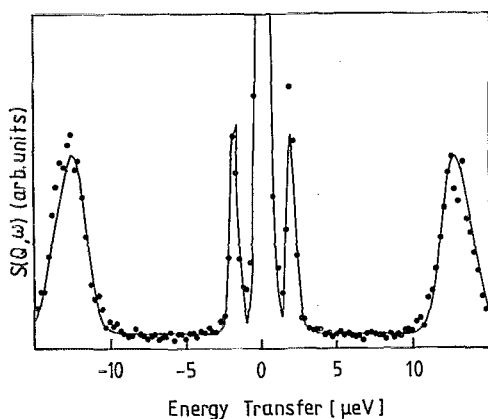


FIG. 2. INS spectrum of $(\text{CH}_3)_3\text{SnCD}_3$, sample I, as measured with the backscattering spectrometer IN10 at ILL. Scattering function $S(Q, \omega)$ in arbitrary units is given as a function of momentum transfer of the neutrons Q , and $\hbar\omega$ is the energy change of neutrons. The instrument resolution is $\delta E = 0.4\ \mu\text{eV}$. The solid line represents the best fit with a model of six inelastic Gaussians and a δ function at zero energy transfer convoluted with the instrumental resolution. Sample temperature $T = 4\ \text{K}$.

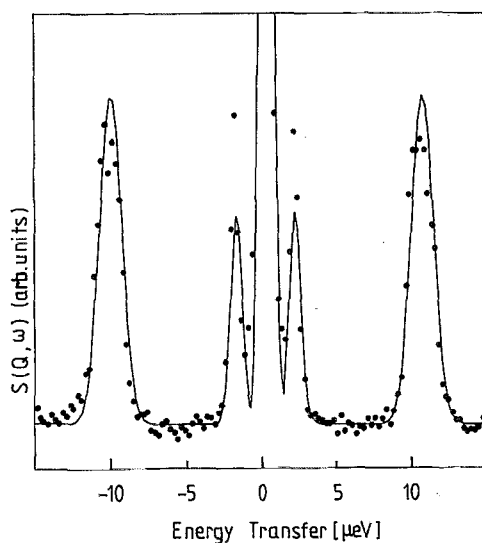


FIG. 3. INS spectrum of $\text{CH}_3\text{Sn}(\text{CD}_3)_3$, sample II. Instrumental setup and coordinates as in Fig. 2. Fitted spectrum: $4\ \text{G} + \text{elastic line}$.

of the neutrons, and $\hbar\omega$ is the energy change of neutrons, is fitted as a function of transferred energy. For comparison, the INS spectrum of $(\text{CH}_3)_4\text{Sn}^{14}$ is reproduced in Fig. 8. The spectra have a common gross structure, namely, one tunnel transition at about $1.8\ \mu\text{eV}$ and another around $11.5\ \mu\text{eV}$ with three times the intensity but varying fine structure. This means that the main tunneling properties of the CH_3 groups in $(\text{CH}_3)_n\text{Sn}(\text{CD}_3)_{4-n}$ as well as in the mixtures $[(\text{CH}_3)_4\text{Sn}]_x[\text{Sn}(\text{CD}_3)_4]_{1-x}$. The measured spectra were fitted by a set of Gaussians convoluted with the experimentally determined resolution function. The tunnel lines shift and broaden or even split up by deuteration. In Table I the tunnel splittings $\hbar\nu_{t,i}$, their linewidths Γ_i , and the intensities of the individual components are presented. The description of some spectral features is not always unique: e.g., sample II could equally well be described at large energy transfer by a doublet line symmetric to $10.5\ \mu\text{eV}$ but with reduced linewidths. To assist the discussion we show the scattering

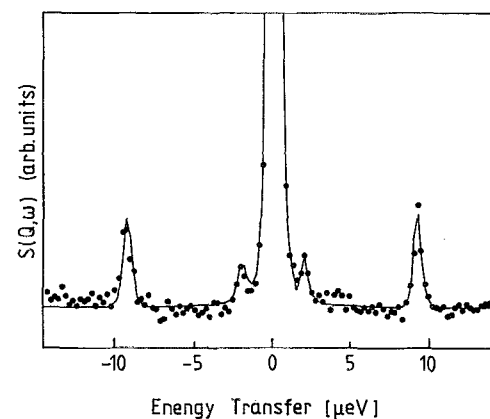


FIG. 4. INS spectrum of isotopic mixture: $[\text{CH}_3\text{Sn}(\text{CD}_3)_3]_{0.10} \times [\text{Sn}(\text{CD}_3)_4]_{0.90}$, sample III. Instrumental setup and coordinates as in Fig. 2. Fitted spectrum: $4\ \text{G} + \text{elastic line}$.

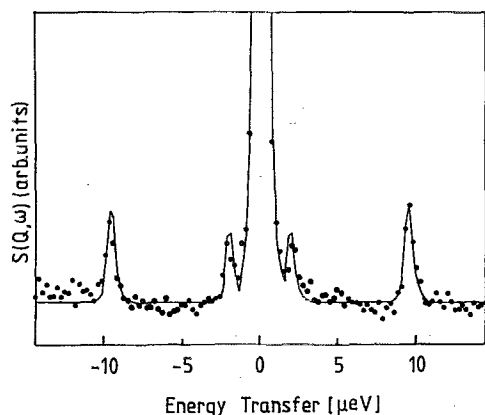


FIG. 5. INS spectrum of isotopic mixture: $[(\text{CH}_3)_4\text{Sn}]_{0.027} \times [\text{Sn}(\text{CD}_3)_4]_{0.973}$, sample IV. Instrumental setup and coordinates in Fig. 2. Fitted spectrum: 4 G + elastic line.

functions fitted to the data in the form of a line diagram in Fig. 9.

IV. DISCUSSION

To begin with, we have to remember the crystal structure and symmetry properties of tetramethyltin in some detail.

The isolated molecule $(\text{CH}_3)_4\text{Sn}$ is a regular tetrahedron with symmetry $\bar{4}3m$. By electron diffraction,^{29,30} all intramolecular carbon-tin distances have been shown to be equal, namely, $d(\text{Sn}-\text{C}^{(n)}) = 214.4$ pm, $n = 1$ to 4.²⁹ The molecular symmetry is proved to be unchanged in the liquid state by IR- and Raman spectroscopy studies.^{31,32}

However, this high molecular symmetry is not maintained in the solid state. The unit cell of $(\text{CH}_3)_4\text{Sn}$ ^{14,16} is shown in Fig. 10 in simplification, that is, only carbon atoms are drawn. Each tetrahedron represents one molecule. The positions of the hydrogen atoms are, unfortunately, not accurately known. The structure essentially shows a cubic packing of tetrahedra within the unit cell. The space group is T_h^6-Pa3 with $Z = 8$ molecules per unit cell (SnI_4 -type struc-

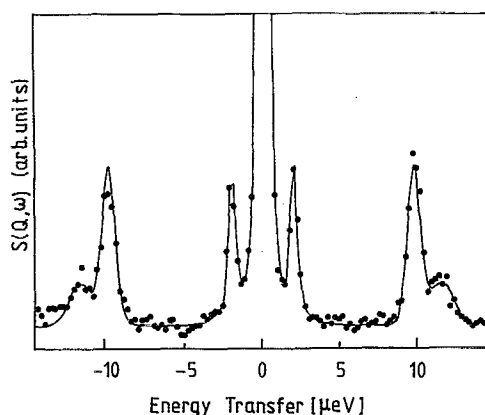


FIG. 6. INS spectrum of isotopic mixture, $[(\text{CH}_3)_4\text{Sn}]_{0.20} \times [\text{Sn}(\text{CD}_3)_4]_{0.80}$, sample V. Instrumental setup and coordinates as in Fig. 2. Fitted spectrum: 6 G + elastic line.

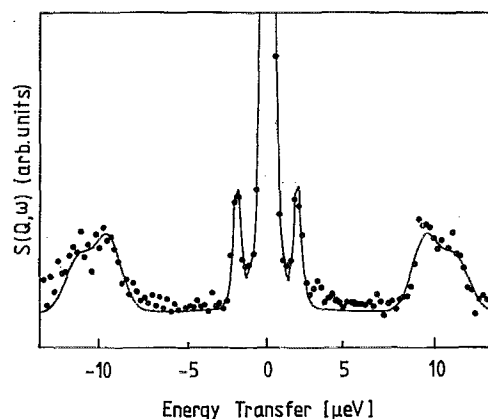


FIG. 7. INS spectrum of isotopic mixture: $[(\text{CH}_3)_4\text{Sn}]_{0.50} \times [\text{Sn}(\text{CD}_3)_4]_{0.50}$, sample VI. Instrumental setup and coordinates as in Fig. 2. Fitted spectrum: 6 G + elastic line.

ture) at $T = 158$ K.¹⁶ the lattice constant is $a = 1119.8$ pm. In this unit cell each tetrahedron is distorted due to a local threefold axis at the molecular centers of mass. One of the four carbon atoms, $\text{C}^{(1)}$, shown as full circles, is located on this axis while the three others (open circles) are off axis, equivalent by symmetry. Two different Sn-C bond lengths result from this symmetry, $d(\text{Sn}-\text{C}^{(1)}) = 210.8$ pm with weight 1, and $d(\text{Sn}-\text{C}^{(n)}) = 214.6$ pm, $n = 2, 3,$ and 4, with weight 3. In the following discussion we denote the $\text{C}^{(1)}$ as $\text{C}(\text{I})$ and $\text{C}^{(n)}$ with $n = 2, 3, 4$ as $\text{C}(\text{II})$. For our problem the carbon-carbon distances are the most relevant quantities. Two different intramolecular carbon-carbon distances result from the molecular distortion: $d(\text{C}(\text{I}) \cdots \text{C}(\text{II})) = 346.8$ pm and $d(\text{C}(\text{II}) \cdots \text{C}(\text{II})') = 350.4$ pm. The shortest intermolecular $\text{C} \cdots \text{C}$ distance is significantly longer and it is between two inequivalent carbon atoms $\text{C}(\text{I})$ and $\text{C}(\text{II})$, namely, $d(\text{C}(\text{I}) \cdots \text{C}(\text{II}))_{\text{inter}} = 399.6$ pm. In the SnI_4 prototype crystal structure intramolecular distances and intermolecular distances $\text{I} \cdots \text{I}$ differ only slightly.³³ In Table II the relevant intermolecular carbon-carbon

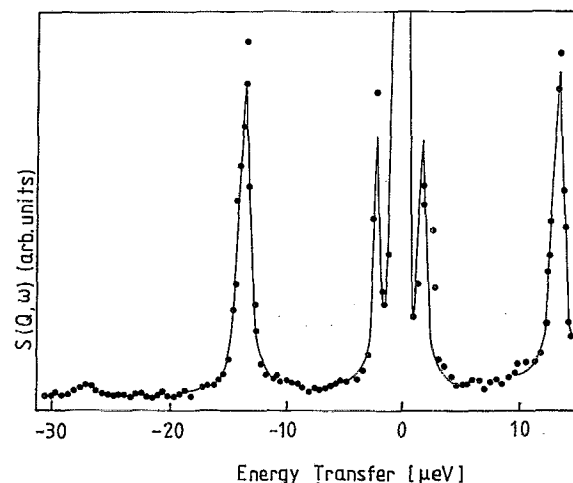


FIG. 8. INS spectrum of tetramethyltin, $(\text{CH}_3)_4\text{Sn}$,¹⁴ sample VII. The solid line is a fit with a Gaussian convoluted with the resolution function. Coordinates as in Fig. 2. Sample temperature $T = 4$ K.

TABLE I. Tunnel splittings $h\nu_{i,i}$, $i = \text{I, II}$, linewidth Γ_i , and multiplicity for the partially deuterated tetramethyltin compounds and isotopic mixture systems studied. The Γ_i values were obtained from the fit results. Values below $0.1 \mu\text{eV}$ mean that the linewidth is mainly determined by the instrumental resolution.

Sample	CD ₃ %	i	$h\nu_{i,i}/\mu\text{eV}$	$\Gamma_i/\mu\text{eV}$	Multiplicity
I. (CH ₃) ₃ SnCD ₃	25	I	1.91	0.09	1:2:1
		II	12.5/13.8	0.97/0.97	
II. CH ₃ Sn(CD ₃) ₃	75	II	1.98	0.10	1:3
			10.5	1.1	
III. [CH ₃ Sn(CD ₃) ₃] _{0.10} [Sn(CD ₃) ₄] _{0.90}	97.5	I	2.06	0.06	1:3
		II	9.43	0.06	
IV. [(CH ₃) ₄ Sn] _{0.027} [Sn(CD ₃) ₄] _{0.973}	97.3	I	1.96	0.06	1:2-3
		II	9.64	0.06	
V. [(CH ₃) ₄ Sn] _{0.20} [Sn(CD ₃) ₄] _{0.80}	80	I	2.00	0.06	1:2:1
		II	9.96/11.8	0.5/1.0	
VI. [(CH ₃) ₄ Sn] _{0.50} [Sn(CD ₃) ₄] _{0.50}	50	I	1.95	0.06	1:2:1.5
		II	10.39/12.32	1.13/1.13	
VII. (CH ₃) ₄ Sn[14]	0	I	1.72	0.01	1:3
		II	13.3	0.4	

distances in (CH₃)₄Sn are given. To a large amount the following spectra can be understood on the basis of the distorted molecule. Intermolecular coupling is able to explain fine details of the spectra.

A. (CH₃)₃SnCD₃ (I)

The INS spectrum of (CH₃)₃SnCD₃ (Fig. 2) is similar to that of (CH₃)₄Sn (Fig. 8). The observation of two tunnel lines with an intensity ratio 1:3 clearly shows that the molecule (CH₃)₃SnCD₃ is statistically oriented with respect to the threefold axis. This means that 75% of CH₃ groups are at the position C(II), 25% are at the position C(I). Such a distribution was expected because the molecule is still very close to a spherical top. The asymmetry is too weak to orient the molecule. Also the entropic contribution to the free ener-

gy works in the direction of a statistical distribution.

The outer strong tunnel line is asymmetric and was fitted by two Gaussians fixed to an intensity ratio 2:1. This leads to an overall intensity distribution of 1:2:1 between the tunnel peaks at $1.91 \mu\text{eV}$, $12.5 \mu\text{eV}$, and $13.8 \mu\text{eV}$, respectively. While the low-energy transition can be described by a resolution line, the two outer lines show a significant width. Figure 11 shows the four possible orientations of the molecule with respect to the C₃ axis induced by the threefold site symmetry. Considering only one molecule, the configurations shown in Figs. 11(b)–11(d) are equivalent. The situation where the molecular and site symmetry axis coincide [Fig. 11(a)] is different from the three other orientations [Figs. 11(b)–11(d)] where they do not. Only protonated methyl groups (open circles) are seen by neutrons. Simple counting shows that the occurrence probabilities are 1:2:1 for all CH₃ groups. This ratio is reproduced in the intensities

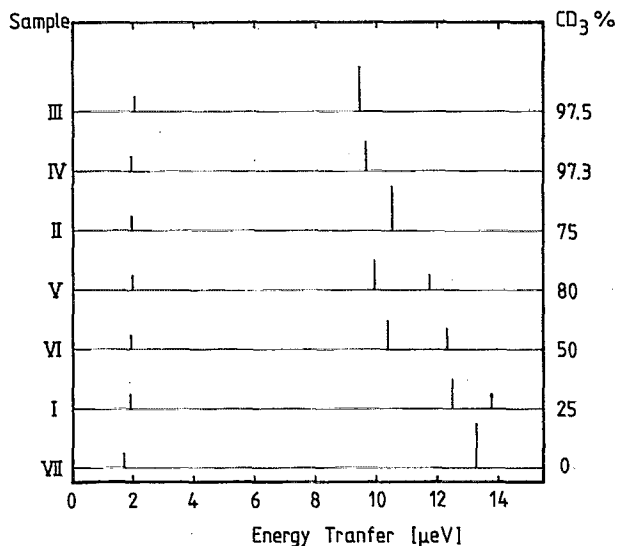


FIG. 9. Line diagram of the tunneling spectra of the investigated compounds.

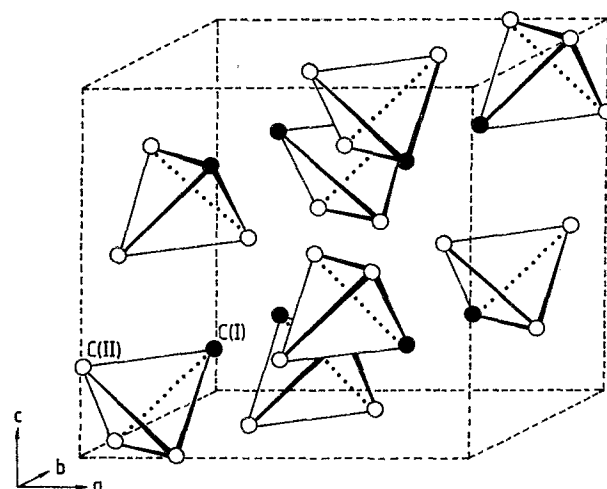


FIG. 10. Crystal structure of protonated tetramethyltin.¹⁴ The tin and hydrogen atoms are not shown. The C(I) atoms (full circles) are represented correctly compared to wrong positions in Fig. 1 of Ref. 14.

TABLE II. Relevant intermolecular carbon-carbon distances in $(\text{CH}_3)_4\text{Sn}$. Space group $T_h^6\text{-Pa}3$, $Z = 8$.^{14,16} C(I) at the axis 3, point position 8c, C(II) at point position 24d (see text and Fig. 10).

Arrangement	d/pm	Multiplicity
C(I)···C(II)	399.6	1:3
	414.9	1:3
	428.5	1:3
C(II)···C(II)'	411.1	1:2
	413.1	1:2
	416.0	1:2
C(I)···C(I)	560.6	1:6

of the tunneling transitions. The $\text{CH}_3(\text{II})$ groups in Fig. 11(a) experience a weaker rotational potential which is reflected in a larger tunnel splitting compared to the $\text{CH}_3(\text{II})$ groups shown in Figs. 11(b)–11(d). In a model of unchanged molecular geometry and intramolecular interactions only, all tunneling lines should be sharp. There is no reason for a distribution of rotational potentials if the only effect of the neighborhood is to create the threefold site symmetry. However, due to the orientational molecular disorder this symmetry is violated and a distribution of somewhat different neighborhoods can be realized. Thus the width of the tunneling lines can only be understood as a result of *intermolecular* interaction. For more details see below.

B. $\text{CH}_3\text{Sn}(\text{CD}_3)_3$ (II)

Qualitatively, the INS spectrum of $\text{CH}_3\text{Sn}(\text{CD}_3)_3$ (Fig. 3) resembles that of $(\text{CH}_3)_4\text{Sn}$ and of $(\text{CH}_3)_3\text{SnCD}_3$. There is an inner tunneling line at $1.98 \mu\text{eV}$ and an outer, broadened one at $10.5 \mu\text{eV}$. The intensity ratio of the two lines is 1:3. The explanation of the spectrum is essentially the same as for $(\text{CH}_3)_3\text{SnCD}_3$. The possible orientations of the $\text{CH}_3\text{Sn}(\text{CD}_3)_3$ molecule with respect to a fixed threefold axis are shown in Fig. 12. In analogy to the above discussion

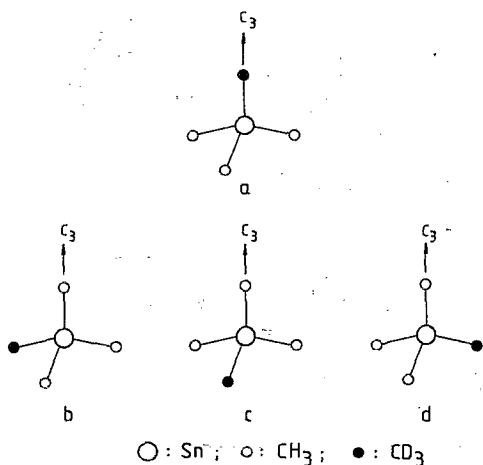


FIG. 11. The four possible orientations of the $(\text{CH}_3)_3\text{SnCD}_3$ molecule with respect to the threefold axis C_3 of the lattice site. Hydrogen atoms are not shown; (b), (c), and (d) are equivalent because of the C_3 symmetry of the molecule (see text).

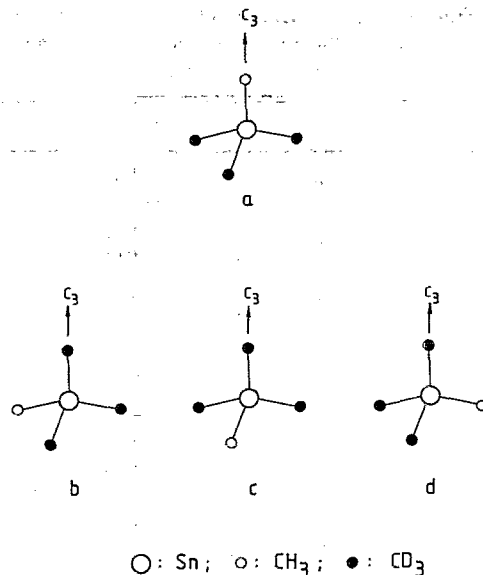


FIG. 12. The four possible orientations of the $\text{CH}_3\text{Sn}(\text{CD}_3)_3$ molecule with respect to the threefold axis C_3 of the lattice site. Hydrogen atoms are not shown.

one sees immediately that the model of noninteracting molecules would yield a single, sharp tunneling line. The appreciable width of this line at $10.5 \mu\text{eV}$ again is only understandable, assuming considerable intermolecular interactions. It was a hope that mixed molecular systems, where the molecules adopt the local site symmetry by distortion, would tell more about this intermolecular interaction.

C. Mixtures $[\text{CH}_3\text{Sn}(\text{CD}_3)_3]_{0.10}[\text{Sn}(\text{CD}_3)_4]_{0.90}$ (III), and $[(\text{CH}_3)_4\text{Sn}]_x[\text{Sn}(\text{CD}_3)_4]_{1-x}$; $x = 0.027$ (IV), 0.20 (V), and 0.50 (VI)

1. Global features

Neglecting the fine structure of the spectrum at large energy transfers (which will be discussed in Sec. IV C 2) the gross features of these spectra are similar to those of the previous samples: There is an inner tunneling line with $h\nu_{t,1}$ around $2.0 \mu\text{eV}$, which belongs to $\text{CH}_3(\text{I})$ groups located on the threefold axis of the molecule, and transitions between 9.4 and $13.3 \mu\text{eV}$, belonging to $\text{CH}_3(\text{II})$ groups. The integrated intensity ratios are roughly 1:3 in agreement with the occurrence ratios of the two species. Low intensities for sample III, $[\text{CH}_3\text{Sn}(\text{CD}_3)_3]_{0.10}[\text{Sn}(\text{CD}_3)_4]_{0.90}$, and sample IV, $[(\text{CH}_3)_4\text{Sn}]_{0.027}[\text{Sn}(\text{CD}_3)_4]_{0.973}$, and especially the overlap of the wings of the elastic line with the inner tunneling transition prohibited a more accurate determination of the intensity ratios for these two samples.

Considering the spectra of all isotopic mixtures III–VI, we find that the reduction of the molecular symmetry from the gas phase symmetry $43m$ to $3m$ is, in rough approximation, still dominating the overall shape. All other effects are absorbed in a broadening or splitting and a shift of the tunneling lines (see Table I). In Fig. 13 we have plotted the splitting of the centers of the tunneling lines versus the CD_3 concentration. It can be seen that the inner tunneling line, belonging to $\text{CH}_3(\text{I})$ groups, shifts little upwards whereas

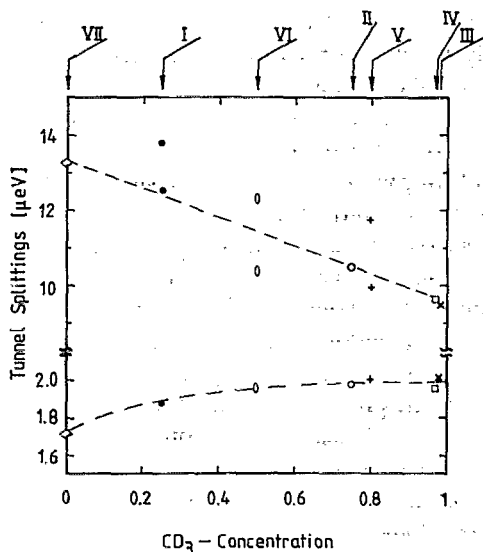


FIG. 13. The tunnel splittings $h\nu$, of all studied tetramethyltin compounds and mixtures (sample I...VI), plotted as a function of the overall CD_3 concentration in the sample. The dashed lines are a guide to the eye only.

the weighted average of the larger tunnel splittings, associated with CH_3 (II) groups decreases appreciably with increasing CD_3 concentration.

This latter behavior has been already observed in various mixed isotopic systems.²⁴ Two effects are responsible for the increase of rotational potentials in deuterated materials. At first, deuterated compounds usually have lattice parameters a different from that of the protonated analog. The lattice parameters a of $(\text{CH}_3)_4\text{Sn}$ and $\text{Sn}(\text{CD}_3)_4$ have been measured simultaneously in the temperature range $20 < T/\text{K} < 190$ by neutron diffraction using a twin cell on the SV4 spectrometer at the KFA Jülich. The temperature dependences of lattice constants a , which are given in Fig. 14, were approximated by power series

$$\begin{aligned} a[(\text{CH}_3)_4\text{Sn}]/\text{pm} &= f(T) \\ &= 0.4412 T^{-1}/\text{K}^{-1} + 11.090 \\ &\quad + 3.9 \times 10^{-4} T/\text{K} \\ &\quad + 3.7 \times 10^{-6} T^2/\text{K}^2, \end{aligned}$$

and

$$\begin{aligned} a[\text{Sn}(\text{CD}_3)_4]/\text{pm} &= f(T) \\ &= 0.4412 T^{-1}/\text{K}^{-1} + 11.073 \\ &\quad + 3.9 \times 10^{-4} T/\text{K} \\ &\quad + 3.7 \times 10^{-6} T^2/\text{K}^2. \end{aligned}$$

The results show that $a[(\text{CH}_3)_4\text{Sn}] > a[\text{Sn}(\text{CD}_3)_4]$ at constant temperature. The extrapolation of the curves give the lattice parameters a at $T = 0 \text{ K}$: $a[(\text{CH}_3)_4\text{Sn}] = 1111.7 \text{ pm}$ and $a[\text{Sn}(\text{CD}_3)_4] = 1110.1 \text{ pm}$, respectively. The change of lattice parameter with deuteration x_D in partially deuterated samples or isotopic mixtures is often assumed to be linear (Vegard's law) and is expressed by

$$a(x_D) = a(x_D = 0) + [a(x_D = 1) - a(x_D = 0)] x_D. \quad (2)$$

With the lattice parameter the intermolecular distances d_i

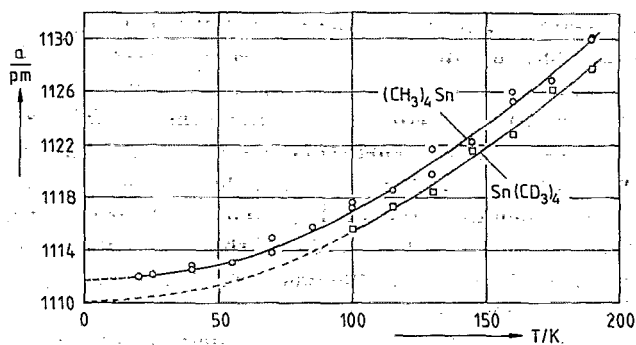


FIG. 14. The temperature dependence of lattice parameters a [$(\text{CH}_3)_4\text{Sn}$] and $a[\text{Sn}(\text{CD}_3)_4]$ measured in the temperature range $20 < T/\text{K} < 190$ by neutron diffraction on the SV4 spectrometer in Jülich.

change. The intra- and intermolecular interactions of the methyl groups in $(\text{CH}_3)_x\text{Sn}(\text{CD}_3)_{4-x}$ are multipole interactions that can be described by power functions d_i^{-n} .^{34,35} As a consequence of reduced distances, the CH_3 groups experience a stronger rotational potential if incorporated in the $\text{Sn}(\text{CD}_3)_4$ matrix and thus the tunnel splitting becomes smaller with increasing concentration of CD_3 groups (see Fig. 13). We emphasize that the contraction of the lattice constant is not due to changes of the intramolecular distances $\text{Sn}-\text{C}$ or $\text{C}-\text{D}$ in the deuterated molecule but it certainly originates from a change of the intermolecular distances. It is likely, however, that the intramolecular $\text{C}\cdots\text{C}$ distances may change too, due to a second-order distortion of the molecule.

The second quantity which determines the strength of the interaction potential beside the intermolecular distances is the multipole moment of the methyl group. In a given potential the CD_3 group has a lower lying ground state than the CH_3 group. This leads to a stronger localization and an increased multipole moment of the CD_3 group. Thus, inevitably, the multipole interactions increase with decreasing CH_3 concentration in mixtures $(\text{CH}_3)_x\text{Sn}/\text{Sn}(\text{CD}_3)_4$.

According to the Lennard-Jones (6-12) pair potential function the rotational potential is a function of the intermolecular distances. For short distances the repulsive interaction is most important and thus

$$V_{\text{rot}} \approx r^{-12}. \quad (3)$$

The rotational potentials thus scale as

$$V_{\text{CD}_3} = (a_H/a_D)^{-12} V_{\text{CH}_3} = 1.0175 V_{\text{CH}_3} \quad (4)$$

by taking $a_H = a[(\text{CH}_3)_4\text{Sn}]$ and $a_D = a[\text{Sn}(\text{CD}_3)_4]$ at $T = 0 \text{ K}$. The change of the tunnel splitting caused by the reduction of lattice parameters according to Eq. (4) should be only $0.8 \mu\text{eV}$ ($13.3 \mu\text{eV} \rightarrow 12.5 \mu\text{eV}$), however. The observed tunnel splitting $h\nu_{\text{II}}$ in the sample III $\{[(\text{CH}_3)_x\text{Sn}(\text{CD}_3)_{4-x}]_{0.10}[\text{Sn}(\text{CD}_3)_4]_{0.90}\}$ with smallest CH_3 concentration is $9.64 \mu\text{eV}$. This shows clearly that the change of the lattice parameters explain only a part of the shift of the tunneling line. The remaining difference must be caused by the stronger localization and an increased octopole moment of the CD_3 groups discussed before.

The positive shift of the tunnel splitting of CH_3 (I)

groups is in disagreement with the above arguments. Taking into account the reduction of the tunnel splitting of CH_3 (II) groups this means that the differences between the two types of methyl groups is reduced. Thus the local threefold axis must be less pronounced in the deuterated substance. In other words, the deuterated molecule is less distorted in the solid state than the protonated one. This is consistent with the systematic behavior¹¹ and should show up in diffraction experiments as a smaller difference between bond lengths $d(\text{Sn}-\text{C}(\text{I}))$ and $d(\text{Sn}-\text{C}(\text{II}))$.

In close analogy to the partially deuterated compounds $(\text{CH}_3)_n\text{Sn}(\text{CD}_3)_{4-n}$, $n = 1, 3$, the statistical distribution of molecules onto lattice sites in $[(\text{CH}_3)_4\text{Sn}]_x \times [\text{Sn}(\text{CD}_3)_4]_{1-x}$ produces rotational potentials with locally varying strength and symmetry. This disorder is the origin of line broadenings. The broadening is most clearly visible in the sample with maximal disorder, i.e., in case of $x = 0.5$ for the CH_3 (II) lines (Fig. 8 and Table I). There is, at most, a broadening $\delta\Gamma$ of the CH_3 (I) tunneling lines expected but difficult to be resolved since the broadening is proportional to the tunnel splitting $h\nu_t$, for a given potential distribution and $h\nu_{t,1}$ of the CH_3 (I) groups is only about 2 μeV .

2. The fine structure of the CH_3 (II) tunneling line

While the gross features of the tunneling spectra reflect the overall change of the methyl rotational potentials with deuteration, the fine structure of the CH_3 (II) tunneling line contains detailed information on the geometry and strength of intermolecular coupling. This information was only available for the mixed systems where the site symmetry is not conflicting with the lowered molecular symmetry.

For very low concentrations of the protonated species (sample IV, $[(\text{CH}_3)_4\text{Sn}]_{0.027}[\text{Sn}(\text{CD}_3)_4]_{0.973}$, see Fig. 5), the $(\text{CH}_3)_4\text{Sn}$ guest molecule is surrounded by deuterated host molecules only. Thus all methyl groups in the crystal, which are equivalent in the pure compound, have the same surrounding. We observe two sharp tunneling lines. The observation is nearly quantitatively the same for $\text{CH}_3\text{Sn}(\text{CD}_3)_3$ guest molecules (sample III, $[\text{CH}_3\text{Sn}(\text{CD}_3)_3]_{0.10}[\text{Sn}(\text{CD}_3)_4]_{0.90}$, see Fig. 4). With increasing concentration of the guest molecules x_H there appears an increasing probability of having neighboring pairs of protonated tetramethyltin molecules. In the model of statistical occupation of lattice sites this probability is x_H . For an individual CH_3 (II) group this means that some of its intermolecular methyl neighbors have converted to CH_3 . The crystal structure¹⁶ shows that just one of the intermolecular CH_3 (I) groups is especially close to CH_3 (II) (see Table II). This pair consists of two CH_3 groups with a probability x_H while it is mixed protonated-deuterated with a probability $(1 - x_H)$. If there is a significant coupling between these two methyl groups, which, furthermore, must be much stronger than any other intermolecular coupling, then the rotational potential will be different in the pair of purely protonated groups from the mixed pair. The two tunneling lines belonging to the two types of pairs should show an intensity ratio $x_H/(1 - x_H)$. It is exactly this fine structure that evolves from the singlet line of Fig. 5 with increasing

protonation (Figs. 5 and 6). Thus we have confirmed once more—as already in the matrix isolation experiment¹⁷—that there is a significant intermolecular interaction in $(\text{CH}_3)_4\text{Sn}$, which couples different molecules dominantly via an infinite network of pairs of methyl groups.

The tunnel splitting within a $\text{CH}_3 \cdots \text{CH}_3$ pair is reduced by about 20% compared to the mixed pair $\text{CH}_3 \cdots \text{CD}_3$. In terms of the theory of coupled tunneling methyl groups³⁶ this corresponds to the case where the interaction potential amplifies the single particle potential. The prototype system for this type of pair interaction is lithiumacetate.²²

The increasing width of the tunneling lines with increasing concentration of the protonated guest molecules shows that the above model which neglects every other interaction beside the pair interaction is somewhat simplified. But it contains all essential features of coupled methyl rotational dynamics in tetramethyltin.

V. CONCLUSION

An insight into the complex intra- and intermolecular interactions between methyl groups in tetramethyltin was given by analyzing the tunnel spectra of partially deuterated and mixed protonated/deuterated samples. Especially the latter samples, in which no disturbing orientational disorder is present, yielded detailed results. The distortion of the molecule in the solid state is reduced with increasing deuteration. The coupling between different molecules is mediated via pairs of methyl groups. Further progress in separating the individual contributions to the methyl groups rotational potential (intra- and intermolecular interactions; single particle-coupling terms) could be obtained by applying external pressure to the tetramethyltin mixtures. The usefulness of such experiments has been shown.¹² Furthermore, an accurate and detailed knowledge of the crystal structure at low temperature and as a function of deuteration could provide an improved understanding.

ACKNOWLEDGMENTS

This work was supported by the Bundesministerium für Forschung und Technologie, Project No. 03WS1DAR1. We are grateful to Dr. A. Heidemann, Dr. H. Blank, and Dr. S. Mahling-Ennanoui of the Institut Laue-Langevin for their help with the high resolution INS experiments.

¹W. Press, in *Springer Tracts in Modern Physics*, edited by G. Höhler (Springer-Verlag, Berlin, 1981).

²M. Prager, W. Press, and K. Roessler, *J. Mol. Struct.* **60**, 173 (1980).

³Y. Ozaki, Y. Kataoka, and T. Yamamoto, *J. Chem. Phys.* **73**, 3442 (1980).

⁴G. J. Kearly, H. Blank, and J. K. Cockcroft, *J. Chem. Phys.* **86**, 5989 (1987).

⁵M. Prager, *J. Chem. Phys.* **89**, 1181 (1988).

⁶D. Cavagnat, A. Magerl, C. Vettier, and S. Clough, *J. Phys. C* **19**, 6665 (1986).

⁷J. R. Durig, S. M. Craven, and J. Bragin, *J. Chem. Phys.* **52**, 2046 (1970).

⁸J. A. Ripmeester, S. K. Gary, and D. W. Davidson, *J. Chem. Phys.* **67**, 2275 (1977).

⁹E. C. Reynhardt, J. C. Pratt, and A. Watton, *J. Phys. C* **19**, 919 (1986).

¹⁰P. S. Allen and A. Cowking, *J. Chem. Phys.* **47**, 4286 (1967).

¹¹W. Müller-Warmuth, K.-H. Duprée, and M. Prager, *Z. Naturforsch. Teil A* **39**, 66 (1984).

¹²A.-S. Montjoie, W. Müller-Warmuth, H. Stiller, and J. Stanislawski, *Z.*

- Naturforsch. Teil A **43**, 35 (1988).
- ¹³G. W. Smith, *J. Chem. Phys.* **42**, 4229 (1965).
- ¹⁴M. Prager, K.-H. Duprée, and W. Müller-Warmuth, *Z. Phys. B* **51**, 309 (1983).
- ¹⁵M. Prager and W. Müller-Warmuth, *Z. Naturforsch. Teil A* **39**, 1187 (1984).
- ¹⁶B. Krebs, G. Henkel, and M. Dartmann, *Acta Crystallogr. C* **45**, 1010 (1989).
- ¹⁷M. Prager, and W. Langel, *J. Chem. Phys.* **85**, 5279 (1986) and *J. Chem. Phys.* **90**, 5889 (1989).
- ¹⁸D. Zhang, L. Walz, M. Prager, and Al. Weiss, *Ber. Bunsenges. Phys. Chem.* **91**, 1283 (1987).
- ¹⁹D. Zhang, M. Prager, S.-Q. Dou, and Al. Weiss, *Z. Naturforsch. Teil A* **44**, 151 (1989).
- ²⁰D. Cavagnat, A. Magerl, C. Vettier, and S. Clough, in *Quantum Aspects of Molecular Motions in Solids, Springer Proceedings in Physics* (edited by H. K. Lotsch) (Springer-Verlag, Berlin, 1987), Vol. 17, p. 24.
- ²¹M. Prager, A. Heidemann, and W. Häusler, *Z. Phys. B* **64**, 447 (1986).
- ²²A. Heidemann, H. Friedrich, E. Günther, and W. Häusler, *Z. Phys. B* **76**, 335 (1989).
- ²³F. Fillaux and C. J. Carlile, *Chem. Phys. Lett.* **162**, 188 (1989).
- ²⁴M. Prager and W. Press, *J. Chem. Phys.* **92**, 5517 (1990).
- ²⁵J. Stanislawski, M. Prager, and W. Häusler, *Physica B* **156,157**, 356 (1989).
- ²⁶W. F. Edgell and C. H. Ward, *J. Am. Chem. Soc.* **76**, 1169 (1954).
- ²⁷Da Zhang, Ph. D. thesis (D17), Darmstadt.
- ²⁸P. Pfeiffer and R. Lehnardt, *Ber. Dtsch. Chem. Ges.* **36**, 1054 (1903).
- ²⁹M. Nagashima, H. Fujii, and M. Kimura, *Bull. Chem. Soc. Jpn.* **46**, 3708 (1973).
- ³⁰L. O. Brokway and H. O. Jenkins, *J. Am. Chem. Soc.* **58**, 2036 (1936).
- ³¹S. Biedermann, H. Bürger, K. Hassler, and F. Höfler, *Monatsh. Chem.* **111**, 703 (1980).
- ³²W. F. Edgell and C. H. Ward, *J. Am. Chem. Soc.* **77**, 6486 (1955).
- ³³P. Braud and H. Sackmann, *Z. Anorg. Allg. Chem.* **321**, 262 (1963).
- ³⁴H. Yasuda, *Prog. Theor. Phys.* **45**, 1361 (1971).
- ³⁵J. O. Hirschfelder, C. F. Curtiss, and R. B. Bird, *Molecular Theory of Gases and Liquids* (Wiley, New York, 1954).
- ³⁶W. Häusler and A. Hüller, *Z. Phys. B* **59**, 177 (1985).